耶鲁–南京信息工程大学大气环境中心
Yale-NUIST Center on Atmospheric Environment

A Discussion on *The Effect of Mesh Resolution on Convective Boundary Layer Statistics and Structures Generated by Large-Eddy Simulation* by Sullivan

Journal Of the Atmospheric Sciences , 2011

Reporter: Wang Kefei
2015.10.23

Outline

- Introduction
- LES equations
- Design of LES experiment
- Overall results
- Results:
  - a. Inertial subrange scaling
  - b. Temperature profile and entrainment statistics
  - c. Convergence of variance statistics
  - d. Spectra analysis
  - e. High-order moments
  - f. Flow visualization
- Summary

Introduction

Large-Eddy simulations (LES) has important role in studying boundary layer dynamics since large-scale parallel computing with increased computer power enables it. The applications include:

- Atmosphere-land interactions;
- Boundary layers with surface water wave effects;
- Weakly stable nocturnal flows;
- Flow in complex terrain

  and so on…

It’s important to examine the quality of LES solutions:

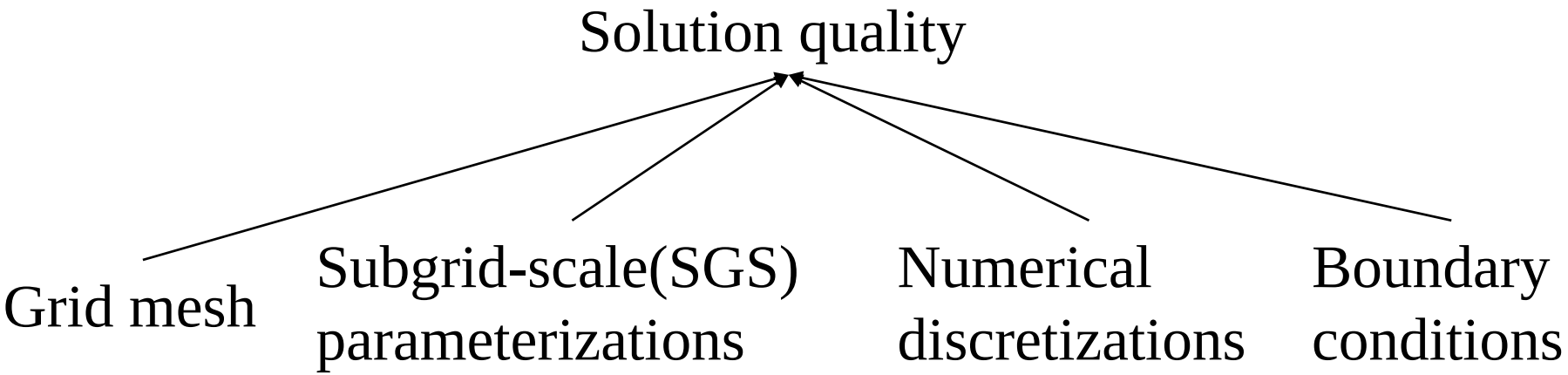

Here, the paper investigate the sensitivity and convergence of LES solutions as the **grid mesh** is substantially varied for a certain choice of SGS model, and the physical problem investigated is a very weakly sheared daytime convective PBL.

LES equations and symbol description

Typical LES model equations for a dry atmospheric PBL under the Boussinesq approximation include:

(a) *transport equation for momentum*:

$$\frac{\partial \overline{\boldsymbol{u}}}{\partial t} + \overline{\boldsymbol{u}} \cdot \nabla \overline{\boldsymbol{u}} = -\mathbf{f} \times \left(\overline{\boldsymbol{u}} - \boldsymbol{U}_g\right) - \nabla \bar{\pi} + \widehat{\boldsymbol{k}} \beta \bar{\theta} - \nabla \cdot \boldsymbol{T} \qquad (1)$$

(b) *transport equation for a conserved buoyancy variable* $(e.g., \textit{virtual potential temperature } \bar{\theta})$

$$\frac{\partial \bar{\theta}}{\partial t} + \overline{\boldsymbol{u}} \cdot \nabla \bar{\theta} = -\nabla \cdot \boldsymbol{B} \qquad (2)$$

(c) *closure expressions for SGS variables* $(e.g., TKE\ e)$

$$\frac{\partial e}{\partial t} + \overline{\boldsymbol{u}} \cdot \nabla e = \mathcal{P} + \mathcal{B} + \mathcal{D} - \varepsilon \qquad (3)$$

Total velocity $\boldsymbol{u} = \bar{\boldsymbol{u}} + \boldsymbol{u}'$

where $\bar{()}$ and $()'$ denote resolved and subgrid fields respectively.

Resolved turbulence fluctuation $\overline{f''} = \bar{f} - \langle \bar{f} \rangle$ and a special case is vertical velocity, $\bar{w} \equiv \overline{w''}$.

where $\langle \cdot \rangle$ denotes ensemble average.

The SGS momentum and scalar fluxes and SGS energy are

$$\mathbf{T} = \overline{u_i u_j} - \bar{u}_i \bar{u}_j \qquad (4a)$$

$$\mathbf{B} = \overline{u_i \theta} - \bar{u}_i \bar{\theta} \qquad (4b)$$

$$e = \frac{\overline{u_i u_i} - \bar{u}_i \bar{u}_i}{2} \qquad (4c)$$

which represent the SGS influence on the resolved field.

Design of LES experiments

- Computation domain is $(L_x, L_y, L_z) = (5120,5120,2048)m$ and the initial inversion height $z_i \sim 1024m$.

Characteristic subgird length scale or LES filter width used in 2D filter $(\Delta f)^3 = \widetilde{\Delta x}\widetilde{\Delta y}\Delta z$, and $(\widetilde{\Delta x}, \widetilde{\Delta y}) = 3(\Delta x, \Delta y)/2$

Table 1. Simulation grid spacings.

Coarse

Run	Grid points	$(\Delta x, \Delta y, \Delta z)(m)$	$\Delta f\,(m)$
A	32^3	(160,160,64)	154
B	64^3	(80,80,32)	77.2
C	128^3	(40,40,16)	38.6
D	256^3	(20,20,8)	19.3
E	512^3	(10,10,4)	9.6
F	1024^3	(5,5,2)	4.8

Fine

- The initial sounding of virtual potential temperature θ has a three-layer structure:

$$\theta(z) = \begin{cases} 300K : 0 < z < 974m. \\ 300K + (z - 974m) \cdot 0.08\ Km^{-1} : 974 < z < 1074m. \\ 308K + (z - 1074m) \cdot 0.003\ Km^{-1} : z > 1074m. \end{cases} \quad (5)$$

A sharp jump in temperature of 8K is imposed over a depth of 100m near the top of the PBL.

- All simulations are started from small random seed perturbations in temperature near the surface.
- The PBL is driven by a constant surface buoyancy flux Q_* and weak geostrophic winds and a fully rough lower boundary.
- The simulations are carried forward for about 25 large eddy turnover time T.

Overall Results

Table 2. Bulk simulation properties.

Run	$z_i(m)$	$z_i/\Delta f$	$z_i/C_s\Delta f$	$w_*(m\ s^{-1})$	w_e/w_*	Re_ℓ	u_*/w_*	$(\delta_b,\delta_t)/z_i$
A	1132	7.2	40	2.07	9.56	238	0.084	(0.74,1.22)
B	1118	14.5	80	2.06	8.45	554	0.091	(0.75,1.18)
C	1099	28.5	158	2.05	6.84	1300	0.090	(0.77,1.12)
D	1092	56.6	314	2.05	5.23	3178	0.087	(0.80,1.09)
E	1088	113.3	630	2.04	5.27	8050	0.084	(0.80,1.07)
F	1099	229.0	1272	2.05	5.16	20600	0.079	(0.80,1.05)

No variant

PBL depth z_i, Deardorff convective velocity scale w_*, entrainment rate w_e, large-eddy Reynolds number at mid-PBL Re_ℓ, friction velocity u_*, bottom and top of the entrainment zone $(\delta_b,\delta_t)/z_i$

Results *a.Inertial subrange scaling*

A fundamental basis of high Reynolds number LES is that the resolved (large eddy) turbulence is independent of SGS influence, namely the SGS viscosity ν_t and scalar diffusivity ν_H.

Define Re_{ℓ} for LES of a convective PBL based on the SGS viscosity ν_t and character velocity and length scale (w_*, z_i)

$$Re_{\ell} = \frac{w_* z_i}{\nu_t} = \frac{w_* z_i}{C_k \Delta f \sqrt{e}} \qquad (6)$$

and

$$\varepsilon = \frac{C_\varepsilon e^{3/2}}{\Delta f}, w_* = \frac{g}{\theta_0} Q_* z_i, C_s = \frac{C_k^{\frac{3}{4}}}{C_\varepsilon^{\frac{1}{4}}} \qquad (7)$$

Leads to

$$Re_{\ell} = \left(\frac{z_i}{\Delta f}\right)^{\frac{4}{3}} \left(\frac{C_\varepsilon}{C_k^3} \cdot \frac{g}{\theta_0} \cdot \frac{Q_*}{\varepsilon}\right)^{\frac{1}{3}} = \left(\frac{z_i}{C_s \Delta f}\right)^{\frac{4}{3}} \left(\frac{g}{\theta_0} \cdot \frac{Q_*}{\varepsilon}\right)^{\frac{1}{3}} \quad (8)$$

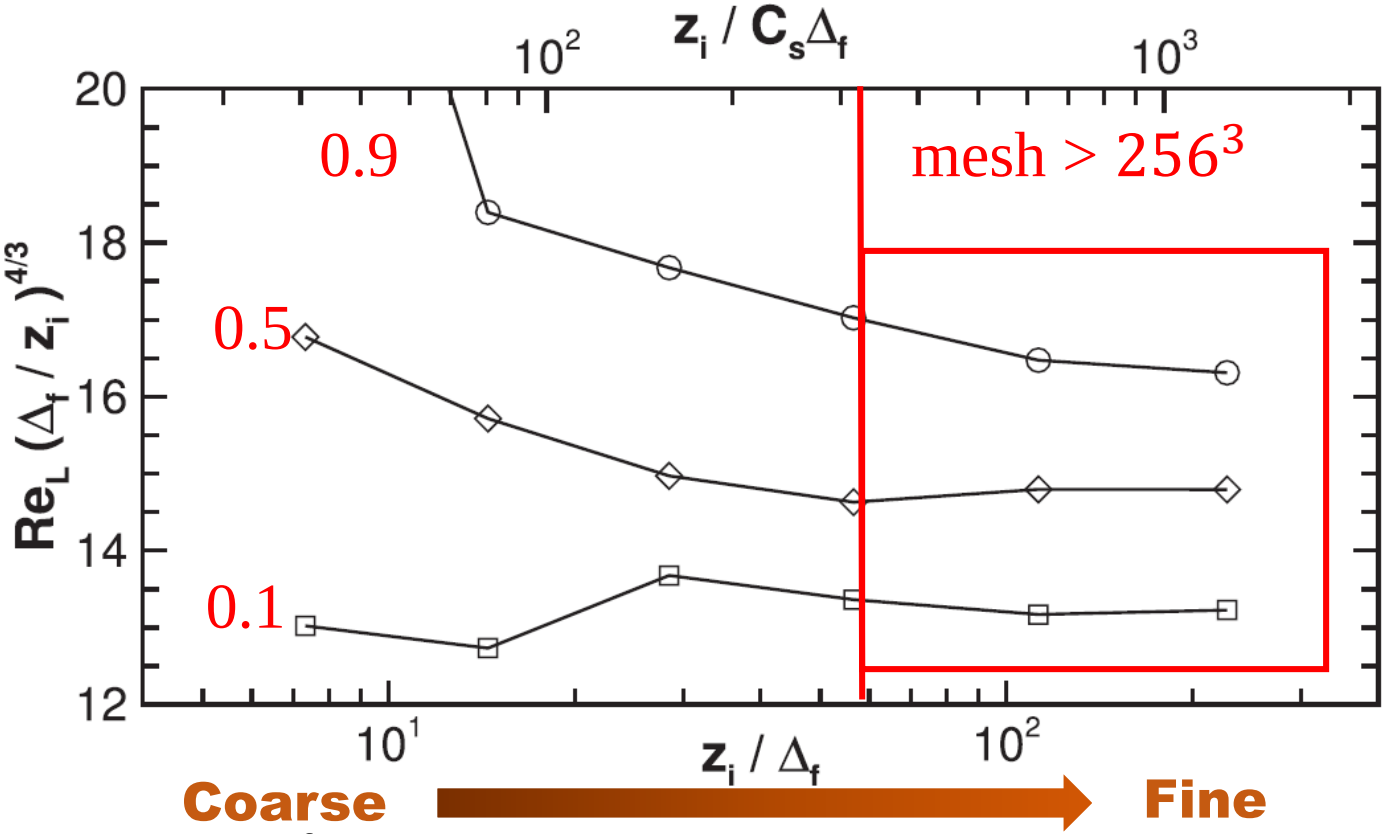

$Re_{\ell} \cdot \left(\frac{\Delta f}{z_i}\right)^{4/3} \approx constant$ if Δf or $C_s \Delta f$ lies in the inertial subrange.

Fig.1 Variation of large-eddy Reynolds number Re_{ℓ} with mesh resolution at heights $\frac{z}{z_i} =$ 0.1,0.5 *and* 0.9

Results *b.Temperature profiles & entrainment statistics*

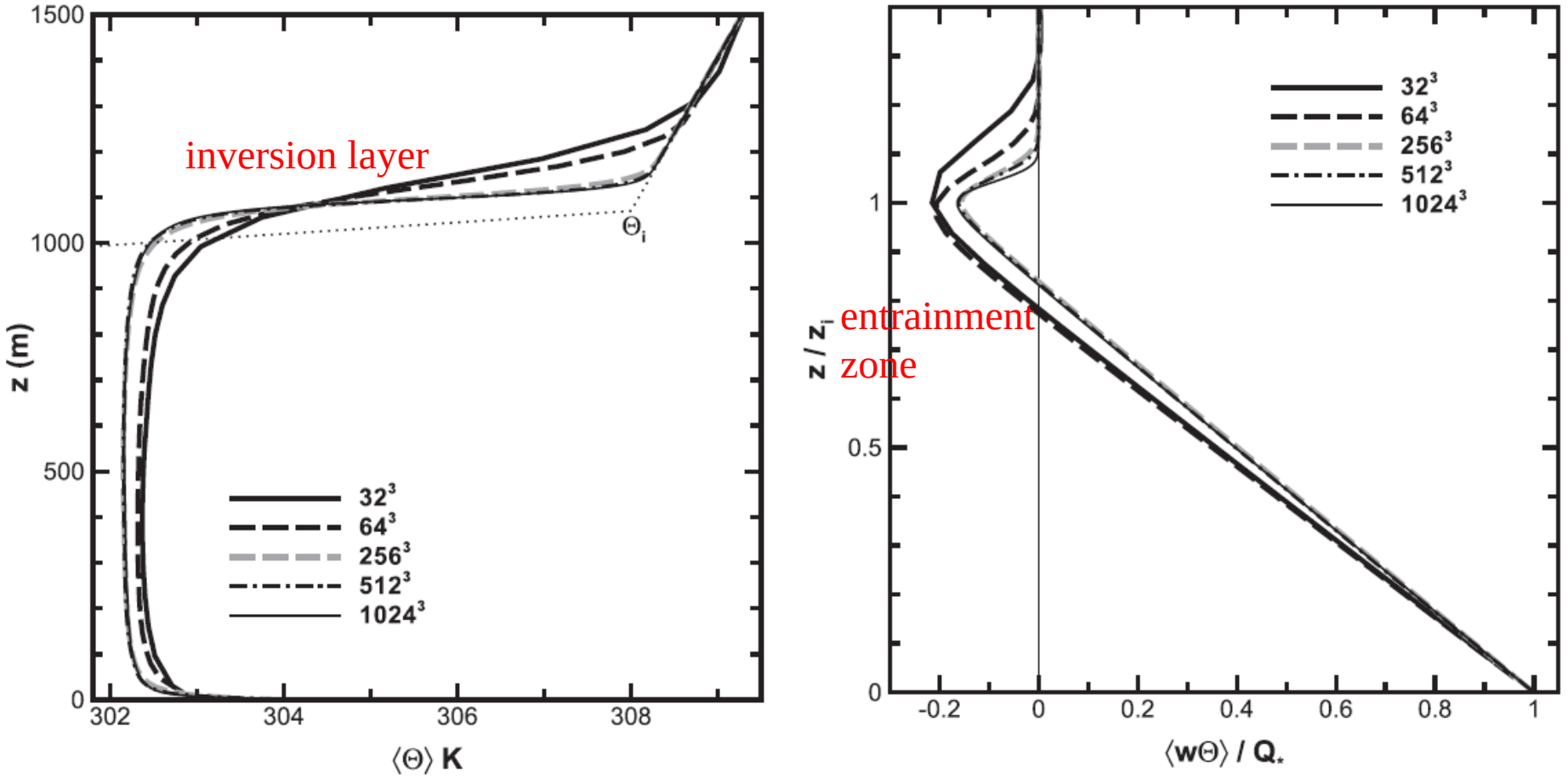

Fig.2 Vertical profile of mean virtual potential temperature $\langle\bar{\theta}\rangle$ and normalized total turbulent temperature flux $\langle\overline{w''\theta''} + \boldsymbol{B}\cdot\hat{\boldsymbol{k}}\rangle/Q_*$ for varying mesh resolution .

Use the maximum vertical gradient in temperature method to determine the PBL height z_i. A critical parameter, the entrainment rate $w_e = dz_i/dt$, is then a function of mesh resolution.

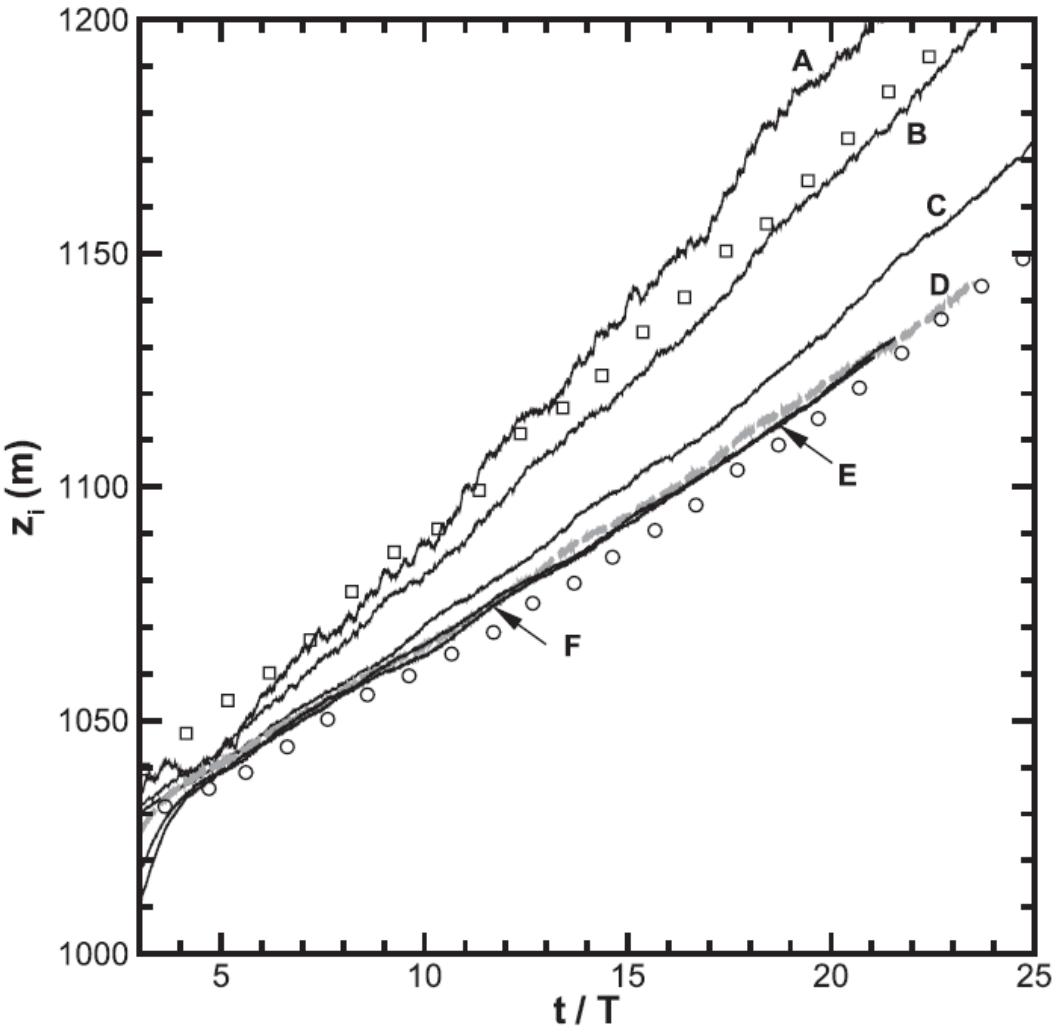

Fig.3 Variation of the boundary layer height z_i with non-dimensional time t/T.

To further expose the coupling between the mean temperature field and turbulence in the entrainment zone, the paper examine the average budget equations for the resolved vertical temperature flux and temperature variance.

>0, M term acts as a sink

$$\frac{\partial}{\partial t}\langle \overline{w''}\,\overline{\theta''}\rangle = \underbrace{-\frac{\partial}{\partial z}\left\langle \overline{w''}^{2}\overline{\theta''}\right\rangle}_{T} \underbrace{-\left\langle \overline{w''}^{2}\right\rangle \frac{\partial\langle\bar{\theta}\rangle}{\partial z}}_{M} \underbrace{+\frac{g}{\theta_0}\left\langle \overline{\theta''}^{2}\right\rangle}_{B} \underbrace{-\frac{1}{\rho}\left\langle \overline{\theta''}\frac{\partial\overline{\pi''}}{\partial z}\right\rangle}_{P} \underbrace{+\mathcal{F}}_{S} \quad (9a)$$

<0 >0

$$\frac{1}{2}\frac{\partial}{\partial t}\left\langle \overline{\theta''}^{2}\right\rangle = \underbrace{-\frac{1}{2}\frac{\partial}{\partial z}\left\langle \overline{w''\theta''}^{2}\right\rangle}_{T} \underbrace{-\langle \overline{w''}\,\overline{\theta''}\rangle \frac{\partial\langle\bar{\theta}\rangle}{\partial z}}_{M} \underbrace{+\mathcal{S}_{\theta}}_{S} \quad (9b)$$

In these equations, T is turbulent transport, M is mean-gradient production, B is buoyant production, P is pressure destruction, and S is a SSG term.

- It is the mean temperature gradient that influences mean temperature flux and temperature variance, and in turn impact the entrainment prediction as well as itself.

- To illustrate the influence of $\partial\langle\bar{\theta}\rangle/\partial z$, additional simulations are added:
  - Simulation D1 uses a 256^3 mesh but sets the filter width Δf equal to the value for the 64^3 with other settings still. (open circle marker in Fig.3)
  - Simulation B1 uses a 64^3 mesh but with no monotone vertical temperature flux. (open square marker in Fig.3)

- Results show that insufficient vertical resolution weakens the inversion and increases the entrainment rate while maintaining nearly the same minimum temperature flux.

Results *c. Convergence of variances statistics*

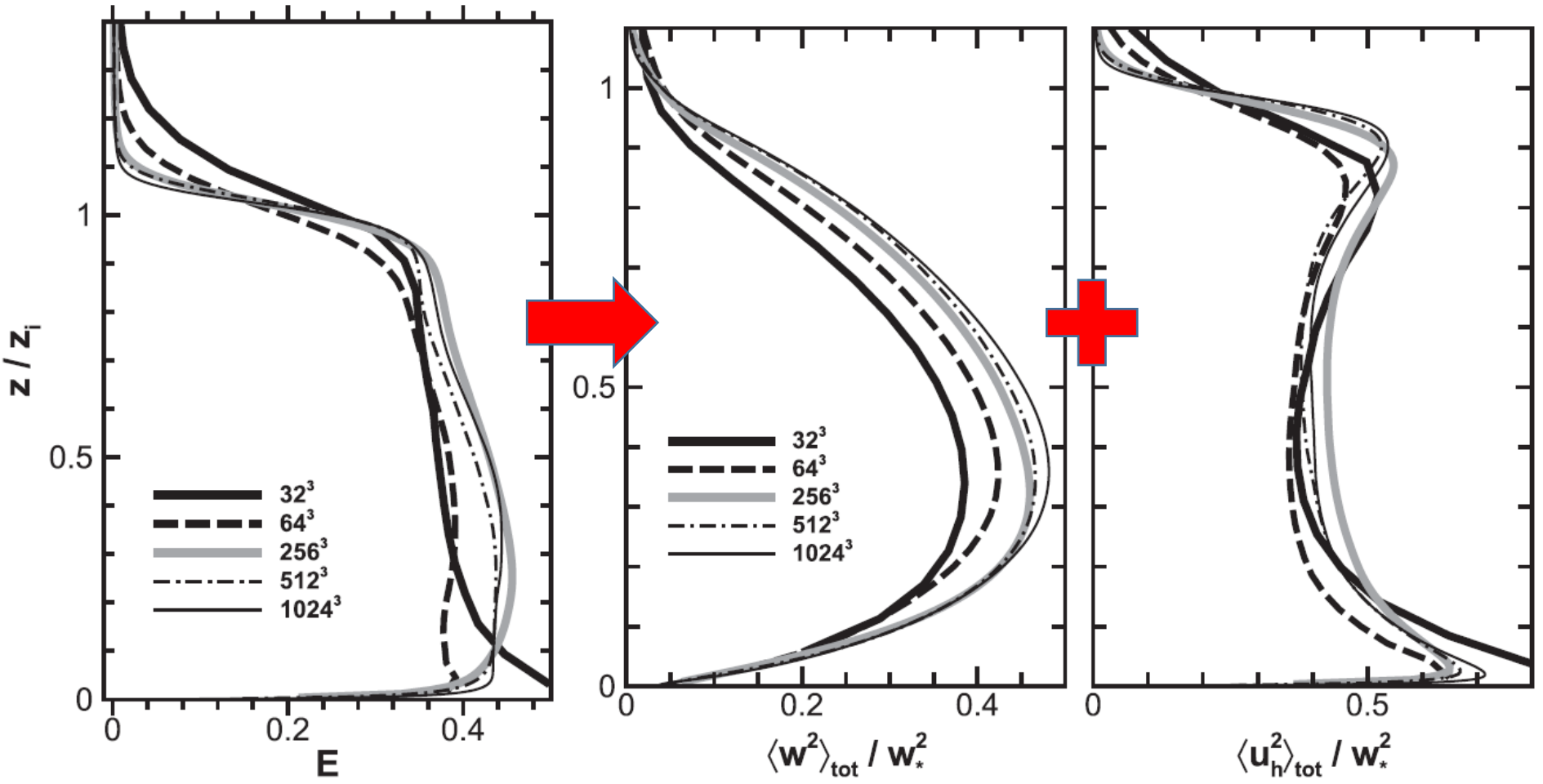

Fig.4 Effect of mesh resolution on the total(resolved plus SGS contributions) TKE(left),total variance of the vertical(middle) and horizontal(right) velocities. TKE is normalized by w_*^2.

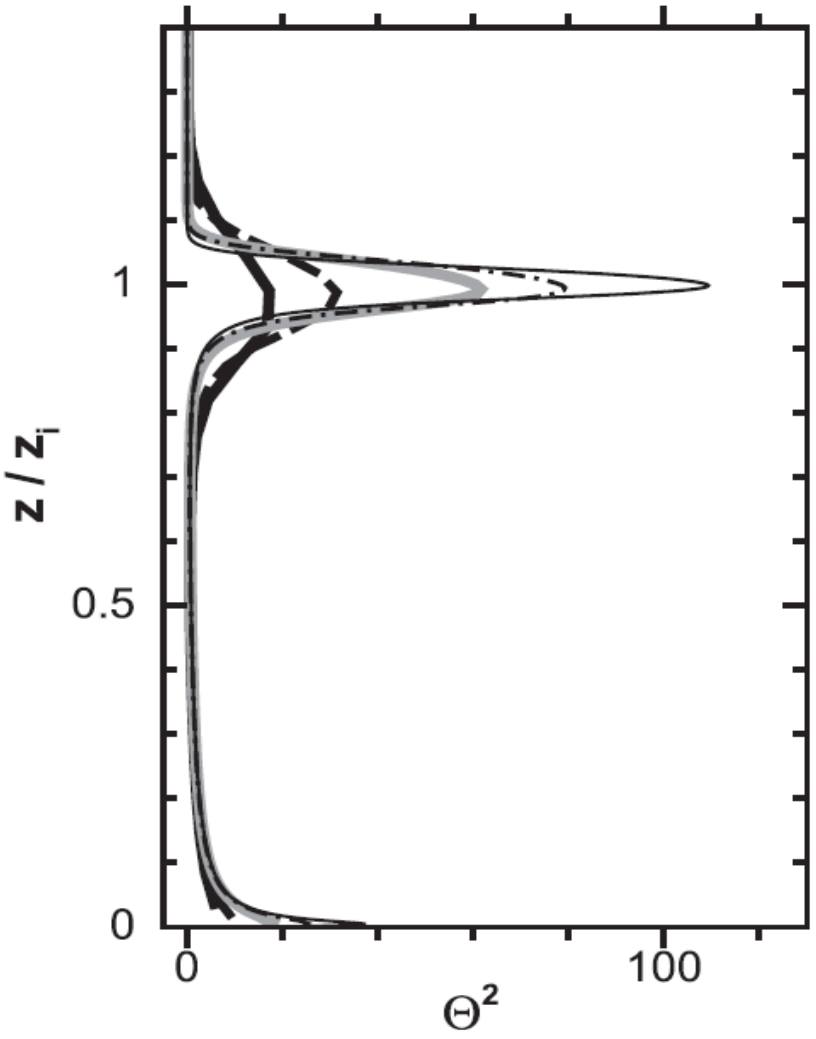

Fig.5 Total temperature variance Θ^2 on different mesh resolution. The temperature variance is normalized by $\Theta_* = Q_*/w_*$.

$$\Theta^2(z) = \left\langle \overline{\theta''}^2 + \varphi \right\rangle / \theta_*^2 \quad (10a)$$

and the SGS variance contribution is diagnosed from:

$$\varphi \sim -\frac{2\ell_f \mathbf{B}\cdot\hat{k}}{C_\theta\sqrt{e}}\frac{\partial\bar{\theta}}{\partial z} \quad (10b)$$

There's no prognostic equation for the SGS temperature variance.

The weaker temperature gradient that develops on the coarse mesh greatly reduces the temperature variance.

Results *d. Spectral analysis*

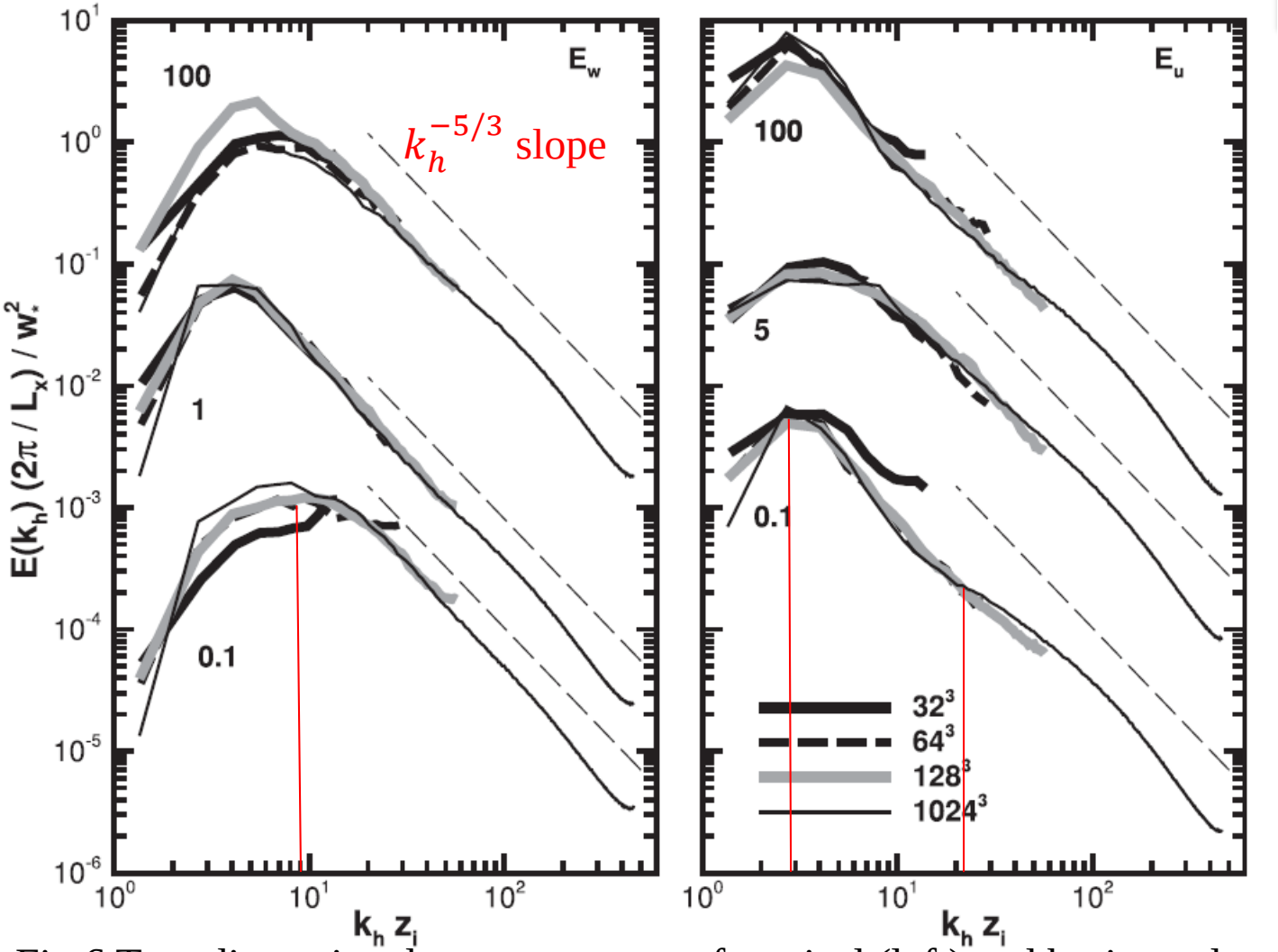

Fig.6 Two-dimensional energy spectra of vertical (left) and horizontal (right) velocity in the PBL for varying meshes. The groups of spectra at the top, middle and bottom are height at 0.9,0.5 and 0.1.

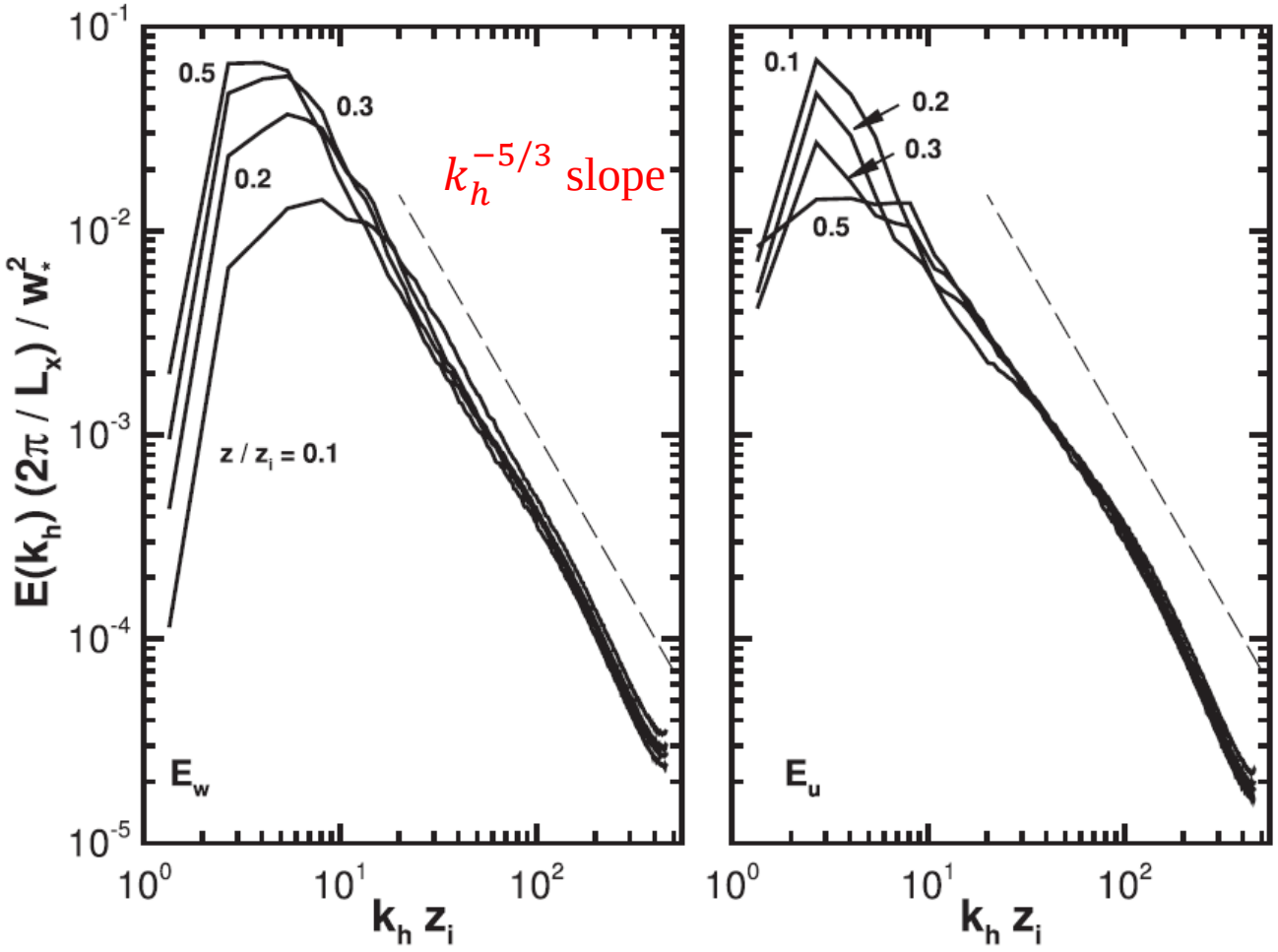

Fig.7 Two-dimensional energy spectrum of vertical(left) and horizontal(right) velocity near the lower boundary at various heights $\frac{z}{z_i}$ =0.1,0.2,0.3 and 0.5 for a simulations with 1024^3 grid points.

Results *e. High-order moments*

Identify the vertical velocity skewness S_w as a critical parameter in boundary layer dynamics, and it is formed by high-order moments.

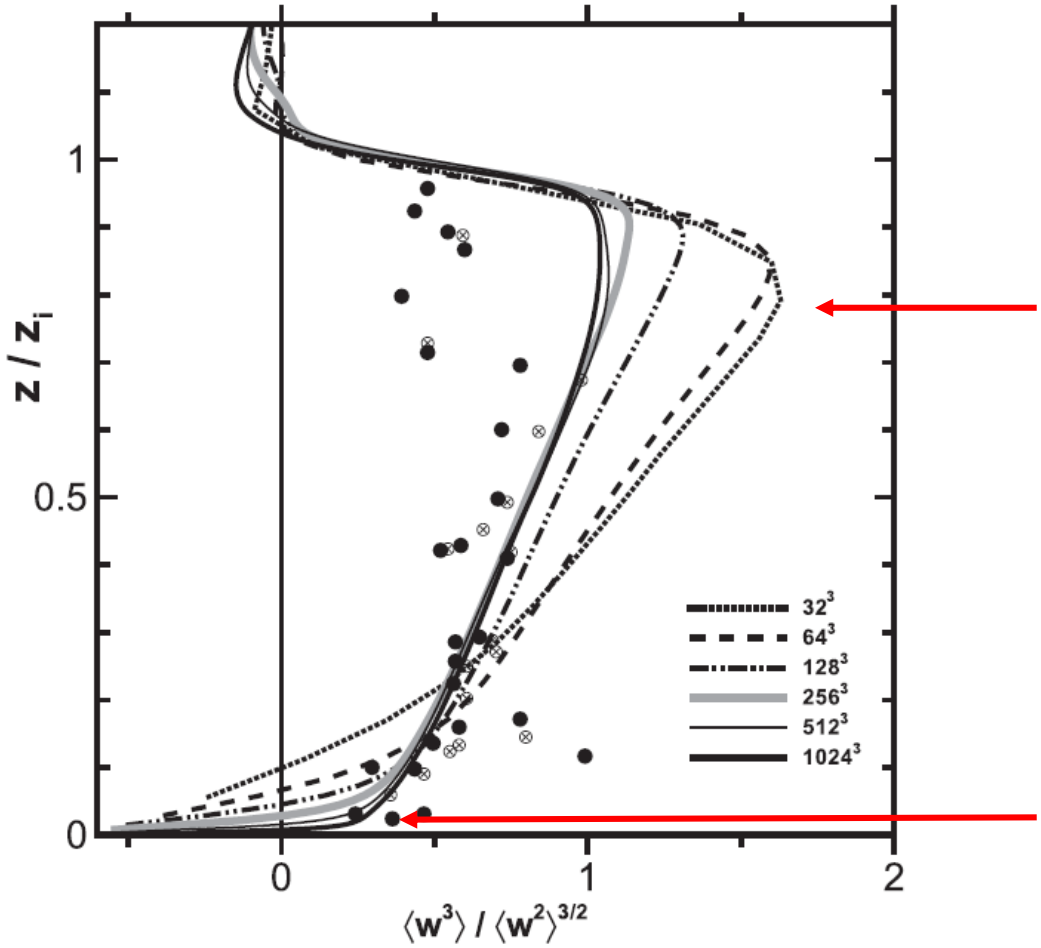

$$S_w = \frac{\langle w^3 \rangle}{\langle w^2 \rangle^{3/2}} \qquad (11)$$

With decreasing grid resolution, $S_{\bar{w}}$ becomes larger and shows a obvious maximum below the inversion.

near the surface $S_{\bar{w}}$ decrease and eventually becomes unrealistically negative on the coarse meshes.

Fig.8 Resolved vertical velocity skewness on different mesh resolution with observations compared.

The interpretation of Fig.8 hinges on the behavior and modeling of the SGS fluxes in LES , since typical LES uses Smagorinsky closures that parameterized fluxes at the second moment level, so there's no clear definition of SGS skewness in LES.

$$S_w = S_{\bar{w}} \frac{(1-\hat{\psi})^{\frac{3}{2}}}{(1-\hat{\phi})} \qquad (12)$$

SGS correction

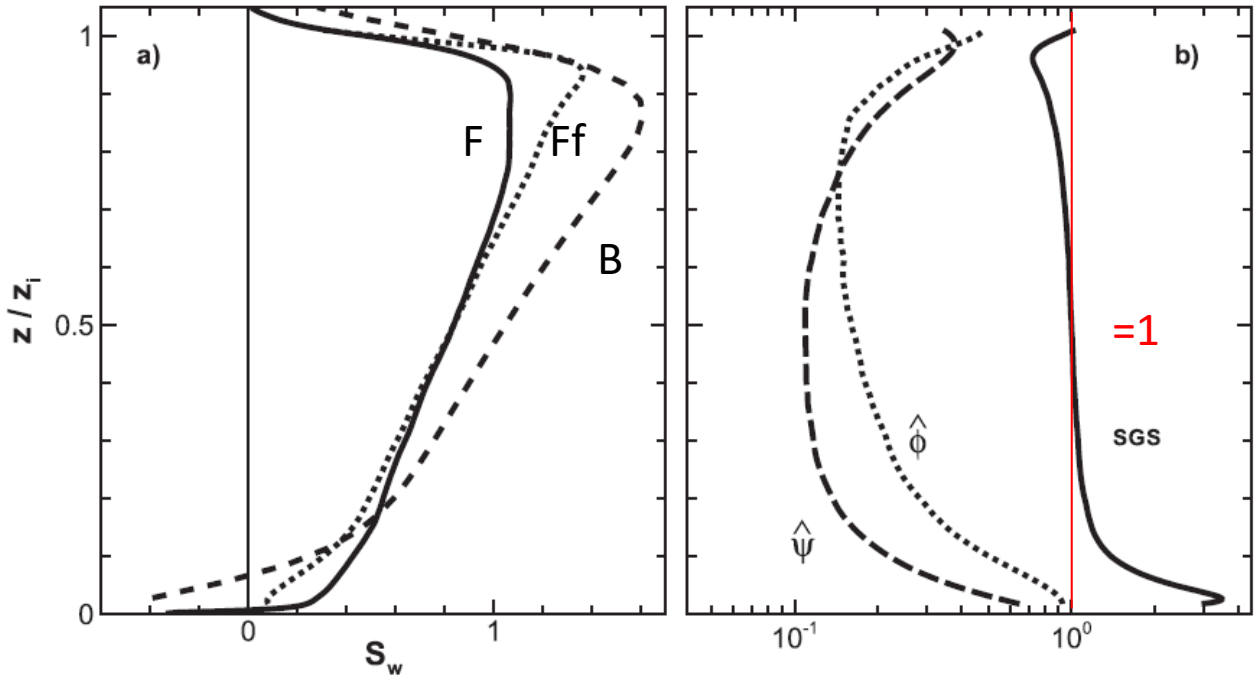

Fig.9 (a)Skewness from simulation F, Ff and B, and (b) SGS moments from Ff.

Hunt et al.(1988) note that Smagorinsky closures assume SGS third-order moment $\hat{\phi} = 0$, as a consequence, coarse-mesh LES results predict erroneous values of skewness.

- When Smagorinsky type closures are used with LES, the resolution ratio $z_i/C_s\Delta f$ needs to be greater than 630 to obtain mesh-independent estimates of $S_{\overline{w}}$.(See Fig.8 simulation E and F)

For other third-order moments

$\gamma_a = \left\langle \overline{w''}^2 \overline{\theta''} \right\rangle$ and $\gamma_b = \left\langle \overline{w''}\ \overline{\theta''}^2 \right\rangle$

There is also a clear mesh dependence in the inversion layer and near the surface.

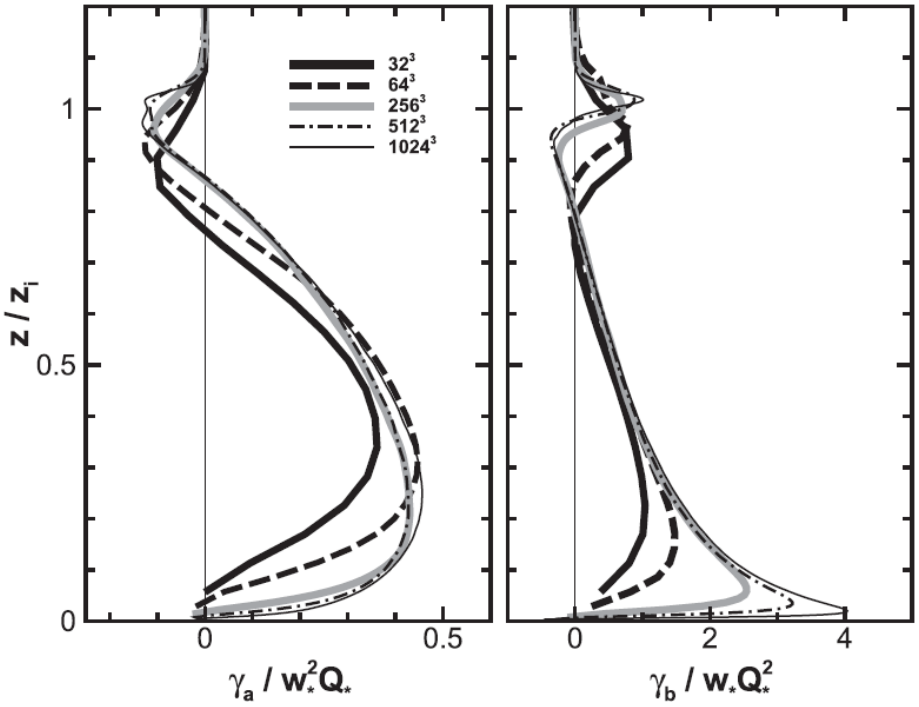

Fig.10 Resolved third-order moments on different mesh resolution.

Results *f. Flow visualization*

Coarse-mesh LES hints at coherent vortices but fine-resolution simulations allow a detailed examination of their dynamics within the larger-scale flow.

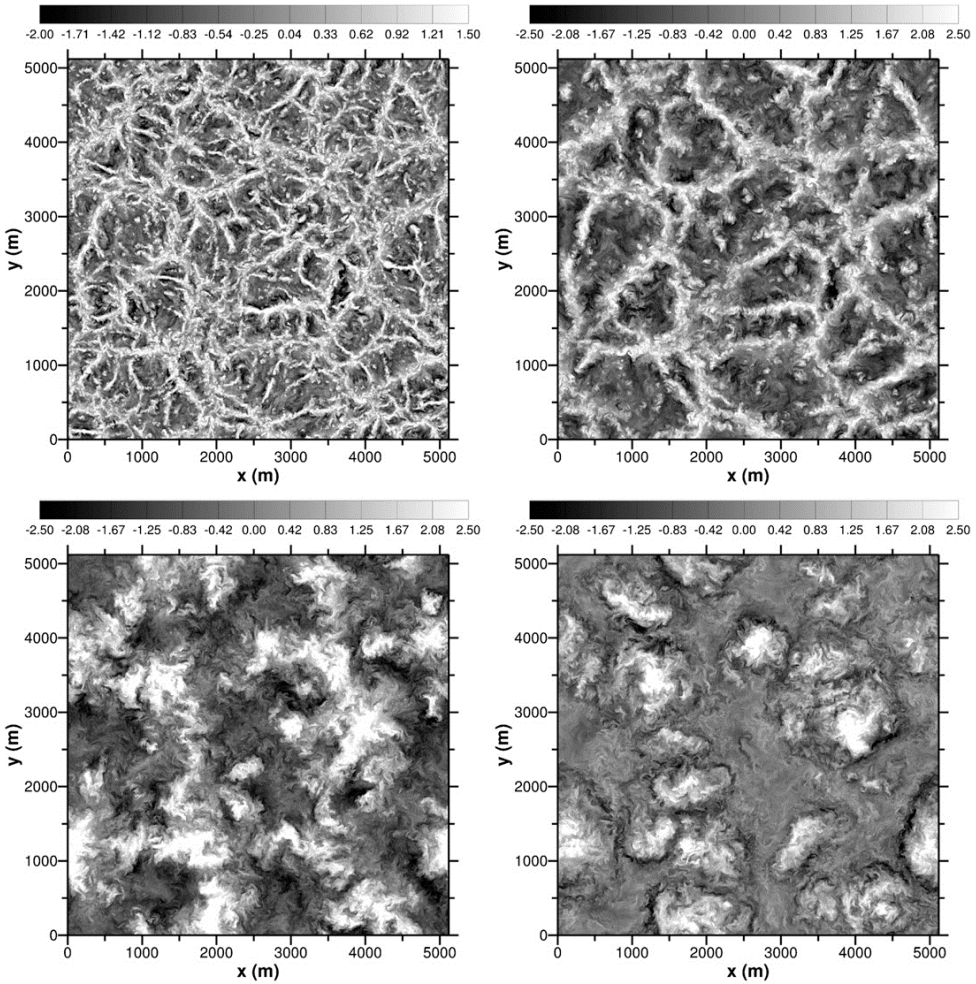

Fig.11 Visualization of the vertical velocity field in a convective PBL at different heights from the F simulation: z/z_i=0.04(top left), 0.1(top right),0.5 and 0.9.

The fine-resolution simulation clearly illustrates the classical formation of plumes in a convective PBL, which represents one aspect of large- and small-scale interaction.

Summary

This code is to carry out a grid sensitivity study of a daytime convective PBL for a wide range of meshes varying from 32^3 to 1024^3. Based on the variation of the second-order statistics, spectra and entrainment statistics we find that the 3D time-dependent LES solutions numerically converge as the mesh is refined.

- For our mesh of 256^3, the ratio $z_i/\Delta f$>60 or $z_i/(C_s\Delta f) > 310$,in this regime, the LES solutions show clear Kolmogorov inertial subrange scaling, which is the basis of most high-Reynolds number subgrid-scale modeling. (results a and d)

- The LES estimates of entrainment velocity become mesh independent when the vertical grid resolution is able to capture both the mean structure of the overlying inversion and the turbulence. (result b)

- Near the rough lower surface and in the entrainment zone , the total (resolved plus subgrid) temperature variance increases with mesh refinement, which is partly a consequence of the SGS model that does not employ a prognostic equation for SGS temperature variance. (result c)

- The mesh dependence of $S_{\overline{w}}$ is a consequence of a Smagorinsky closure that neglects third-order SGS moments of vertical velocity. Simulation with 512^3 mesh points or more are needed to estimate vertical velocity and higher-order moments from the resolved LES flow field. (result e)

- The criterion $z_i/(C_s\Delta f)$>310 proposed here for simulations of convective boundary layers needs to be tested under other meteorological conditions.

Thank you